General Disclaimer

One or more of the Following Statements may affect this Document

- This document has been reproduced from the best copy furnished by the organizational source. It is being released in the interest of making available as much information as possible.

- This document may contain data, which exceeds the sheet parameters. It was furnished in this condition by the organizational source and is the best copy available.

- This document may contain tone-on-tone or color graphs, charts and/or pictures, which have been reproduced in black and white.

- This document is paginated as submitted by the original source.

- Portions of this document are not fully legible due to the historical nature of some of the material. However, it is the best reproduction available from the original submission.

Produced by the NASA Center for Aerospace Information (CASI)

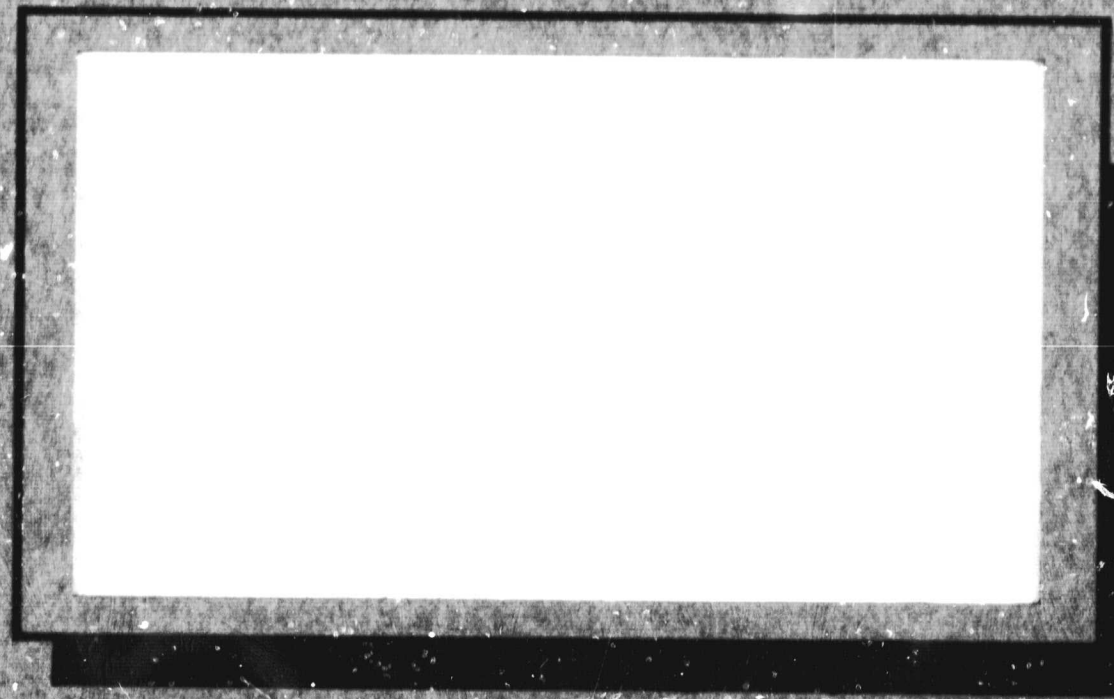

CENTER FOR SPACE RESEARCH
MASSACHUSETTS INSTITUTE OF TECHNOLOGY

N70-11247

(ACCESSION NUMBER) 29 (PAGES) CR-106735 (NASA CR OR TMX OR AD NUMBER)

(THRU) 1 (CODE) 25 (CATEGORY)

FACILITY FORM 602

Pioneer 6 Plasma Measurements in the Magnetosheath

by

Herbert C. Howe Jr.

CSR-P-16 June 1969

Massachusetts Institute of Technology
Center for Space Research
Cambridge, Mass. 02139

Abstract

Measurements of the magnetosheath plasma made by the MIT Plasma Experiment during the outbound passage of Pioneer 6 in the dusk meridian (December 16, 1965) are presented and compared with theoretical predictions for the same region. While the comparison indicates that the plasma flow around the earth agrees in many ways with a gas dynamic model, observed discrepancies in the density ratio across the bow shock and the non-Maxwellian velocity distribution in the magnetosheath warrant further explanation. Magnetosphere and magnetosheath low energy electron measurements indicate a region of anisotropic flux in the magnetosphere near the magnetopause.

Introduction

The flow of plasma in the earth's magnetosheath has been the subject of experimental (Hundhausen et al., 1969; Wolfe et al., 1968, Olbert, 1968) and theoretical (Spreiter et al., 1966) papers. Spreiter et al. (1969) give a comprehensive review of both experimental and theoretical results. By comparing the observations of Wolfe, et al. (1968) with the theory of Spreiter et al. (1966), Spreiter and Alksne (1968) conclude that the magnetosheath flow is described well by gas-dynamic theory. In this paper, the results of the Pioneer 6 M.I.T. measurements of magnetosheath plasma flow are presented and compared with the gas-dynamic theory. While there are some important discrepancies, the comparison tends to confirm the agreement between the experimental results and the theory.

TRAJECTORY AND INSTRUMENTATION

Pioneer 6 was launched at 0731 UT, December 16, 1965, from Cape Kennedy into a heliocentric orbit. The near-earth part of the trajectory lay within 5° of the solar ecliptic plane near the dusk meridian, as shown in Figure 1. The spacecraft was spin stabilized during these observations; and until two days after launch, the spacecraft equatorial plane was tilted about the sun-spacecraft line 38.6° to the solar ecliptic plane. The tilt was counter-clockwise as viewed from the sun, and the spin was clockwise as viewed from the North.

Details of operation of the MIT plasma experiment have been described elsewhere (Lazarus et al., 1966), but the basic mechanism is as follows: The Faraday cup plasma detector measures the flux of particles whose energies lie in an energy/charge range determined by a modulating grid. The cup normal is perpendicular to the spin axis and the width of the angular response of the cup is $\pm 20°$ in the plane normal to the spin axis and $\pm 60°$ perpendicular to this plane. On every other revolution, the cup measures the flux in one energy range (channel) in each of 13 angular sectors. The channels and sectors are summarized in Figure 2. The measurement of a positive ion energy-angular spectrum is initiated every minute and requires 30 seconds to complete. During each positive ion spectrum measurement, flux in one of the four electron energy channels is measured, thus one

complete electron energy-angular spectrum is obtained every four minutes. The circular collector plate is split in half so that the fluxes from above and below the spacecraft equatorial plane may be measured separately to give the component of plasma velocity perpendicular to this plane.

METHOD OF ANALYSIS

To determine the average velocity and the density of the protons and to parameterize the velocity spread around the average velocity, the response of the cup to a model plasma was calculated and compared with the observations. For most of the calculations in this paper, it was assumed that the protons were described by an isotropic convected Maxwellian distribution

$$f(\underset{\sim}{v}) = \frac{n}{\pi^{3/2}\ \omega_0^3}\ e^{-(\underset{\sim}{v}-\underset{\sim}{v}_b)^2/\omega_0^2}$$

characterized by an average (bulk) velocity $\underset{\sim}{v}_b$, a thermal speed ω_o and a number density n. The thermal speed is the most probable speed of the Maxwellian speed distribution and is related to the temperature by $1/2\ m\omega_o^2 = kT$, where m is the particle mass and T is the absolute temperature.

By varying the bulk velocity and thermal speed at an assumed density, it was possible to calculate energy-angular spectra which were proportional to those observed. The density was found

by scaling the assumed density by the ratio of the observed to calculated fluxes.

For several spectra, a bi-Maxwellian distribution was used. This distribution is similar to the one above, but it is characterized by one thermal speed along the direction of the $\underset{\sim}{B}$ field and another perpendicular to that direction. During the magnetosheath crossing, the observed magnetic field direction (Ness et al., 1966) was within 30° of the bulk velocity direction. To facilitate calculations, the bulk velocity was taken as the direction of the parallel thermal speed. The results of the analysis of these spectra indicated that the ratio of the parallel to perpendicular thermal speeds was constant throughout the traversal. Since the isotropic fit was made to the currents in the peak angular sectors, the resulting thermal speed was that corresponding to the parallel thermal speed of the bi-Maxwellian distribution. Comparisons of the isotropic and bi-Maxwellian fits to identical spectra showed that the bulk velocities and thermal speeds from the two distributions agreed to within 2 km/sec. The magnetosheath thermal speeds reported in this paper are those parallel to $\underset{\sim}{v}_b$ (and $\underset{\sim}{B}$) unless explicit reference to a perpendicular thermal speed is made. An example of a bi-Maxwellian fit to an observed spectrum is shown in Figure 3.

In the magnetosheath, electron flux was measurable only in the lowest electron energy channel. Also, electron angular measurements were possible only when the cup faced away from the

sun, i.e., in angular sectors 9-13, (see Figure 2) because the instrument was flooded with photoelectrons whenever it faced the sun. Since the electron data were insufficient to determine as many parameters as were used to characterize the proton spectra, it was assumed that the proton and electron bulk velocity, number density, and flow direction were equal. By then using an isotropic (one thermal speed) Maxwellian model, the observed angular distribution of electrons was satisfactorily explained and an electron thermal speed was derived for each electron spectrum.

Two different regions of electrons were observed inside the magnetopause. In the first region, angularly isotropic fluxes were detected in all four electron channels. An isotropic, Maxwellian model with zero flow velocity was fitted to these spectra (an example of the fit is shown in Figure 5) and values for the electron density and thermal speed were derived. In the second region, angularly-anisotropic fluxes were detected primarily in the lowest electron channel, with currents just above threshold also evident in the next highest channel in some cases. This anisotropy could have been due to either a thermal anisotropy or a large electron bulk velocity. Due to the sparseness of these data, it was not possible to exclude either of these explanations and the data were analyzed under both assumptions.

RESULTS

The non-Maxwellian proton spectra observed in the magnetosheath limit the physical meaning of the derived thermal speeds and introduce a systematic error into the velocities and densities which are derived using an isotropic Maxwellian distribution function. To give some feeling for the size and importance of these discrepancies, we shall first discuss the non-Maxwellian nature of the observed spectra. As the basis for presentation of the results, we shall then compare the bulk velocities, thermal speeds, densities, and flow directions obtained from the data with those predicted by classical gas-dynamic calculations for supersonic flow around a blunt object. Finally, the results from the electron data analysis will be discussed.

From the typical magnetosheath proton spectrum and the Maxwellian approximation to this spectrum presented in Figure 3, it is evident that the magnetosheath proton velocity distribution is non-Maxwellian. The high energy, non-Maxwellian tail is estimated to contain roughly 10% of the total number density. A rough estimate shows that including these particles, the actual bulk velocities and densities should be respectively about 3% and 10% higher than those velocities and densities which were derived on the basis of a Maxwellian model. This systematic error is present in all the magnetosheath proton results reported here, since the high-energy tail was present throughout the magnetosheath.

The angular distribution of particles in the channels containing the high-energy tail indicates that these protons travel in the direction of the bulk flow in the magnetosheath except near the bow shock. 2-3 minutes before crossing the shock into the interplanetary medium, the high energy particles began coming from the direction characteristic of the interplanetary plasma, while the bulk of the plasma continued to flow in the deviated direction observed throughout the magnetosheath. After crossing the shock into interplanetary space, no current was measured in the high-energy tail channels. Apparently, the high energy particles were produced as the solar wind traversed the shock, but they did not immediately flow in the deviated direction characteristic of the bulk magnetosheath plasma.

As mentioned before, it was not possible to explain the angular distribution of the bulk of the protons by using a one-temperature distribution. To obtain the fit shown in Figure 3, it was necessary to choose a thermal speed of 50 km/sec along the direction of the bulk velocity and a speed of 70 km/sec perpendicular to this direction. Thus the temperature perpendicular to the average field direction was about twice that parallel to this direction. This ratio was observed throughout the magnetosheath traversal.

We now proceed to compare the experimental results with theory. The gas dynamic calculations (Spreiter et al., 1966) predict the flow parameters in the magnetosheath on the basis of

those in the incident solar wind. Shortly after passage from the magnetosheath into the interplanetary medium, the measured (incident) plasma parameters were

v_b = 300 Km/sec. n = 15 protons /cm^3

ω_o = 10 Km/sec. B = 3-4 gamma

where v_b, ω_o, n, and B are the bulk velocity, thermal speed parallel to v_b, density, and magnetic field strength, respectively. The incident thermal speed perpendicular to v_b was about 30 km/sec. In the interplanetary medium, the bulk velocity and magnetic field were not parallel and the above thermal speeds do not refer to the direction of the magnetic field. The values of these parameters for the magnetosheath also depend on the solar wind Mach number and on the assumed value of γ, the specific heat ratio. The velocity of a fast wave travelling directly upstream in the solar wind under the above conditions is 15 km/sec, thus the incident Mach number was M_o = 20. Also, γ = 5/3 was arbitrarily chosen as the specific heat ratio. During the magnetosheath traversal, K_p was zero (Lincoln, 1966); and after the shock crossing, the solar wind remained steady. Thus we assume the incident conditions above were constant throughout the traversal.

In performing the gas-dynamic calculations, Spreiter et al.

(1966) first calculated the position of the magnetopause and bow shock. These two boundaries, properly scaled for the above solar wind conditions, are superimposed on the Pioneer 6 trajectory in Figure 1 and the observed boundary crossings are indicated. The magnetopause was crossed only once; but after the spacecraft crossed the shock into the interplanetary medium, the shock moved over it so that the magnetosheath medium was detected again before the spacecraft again crossed the shock and remained in the solar wind. These three crossings took place in less than 30 seconds, thus no information on plasma changes between crossings could be obtained, but the multiple crossings do indicate shock motion.

The observed and theoretical plasma flow directions, measured from the spacecraft-sun line, are also indicated in Figure 1. Both the incident solar wind and magnetosheath plasma were directed roughly 5° north of the solar ecliptic plane, but this small deviation has been ignored in the comparison with theory.

The plasma parameters measured along the trajectory are shown in Figures 4 and 5. As the spacecraft passed from the magnetopause to the bow shock, the bulk velocity and density were observed to increase, while the thermal speed fell slightly. This behavior is in complete agreement with the gas-dynamic calculations. Upon crossing the shock into the interplanetary medium, the bulk velocity increased and changed to the aberrated direction, while the thermal speed and density fell, also in accord-

ance with the model. The discrepancy in the actual ratios of the quantities across the shock will be discussed below.

The results of the electron analysis are shown in Figure 6. Proceeding outward from the earth, three distinct regions (regions A-C in Figure 6), each with a unique type of electron flux, were observed before crossing the bow shock. The first region was observed between 9 R_E and 11.5 R_E and was characterized by angularly isotropic fluxes in all four electron channels. The form of the energy spectra in this region indicates that it was the plasma sheet (Vasyliunas, 1968). This region terminated abruptly at 11.5 R_E where most of the flux began to be measured in the lowest channel. As discussed above, the observed fluxes in this second region could be explained in two ways. First, the observed fluxes could be fitted with a Maxwellian distribution having a pressure of about 300 ev/cm^3 and a temperature anisotropy of $T_{\parallel}/T_{\perp} = 2$, where $T_{\parallel}$ was roughly along the magnetic field direction and the bulk velocity was assumed to be zero. Alternately, the observed fluxes were consistent with a convective electron velocity of roughly 750 km/sec, directed away from the sun along the spacecraft-sun line, and a thermal speed of about 2,500 km/sec. This region was about 1.5 R_E wide and was bounded at the outer edge by the magnetopause. The thermal energy, speed, and temperature in the third region, the magnetosheath, were about 40 ev, 2700 km/sec and 10^5 °K and tended to be higher

near the bow shock. No electrons were observed after crossing the bow shock, due to the lower temperature of the electrons in the solar wind.

DISCUSSION

The magnetosheath traversal of Pioneer 6 was particularly valuable in that it provided a detailed cross section of the magnetosheath plasma in the dusk meridian during particularly quiet conditions. For the period involved, $K_p = 0^+$ and the College magnetograms showed no activity for the entire day. Also, the solar wind remained steady for several days after the traversal. Therefore, the measurements made are probably characteristic of the basic, static interaction between the solar wind and the earth.

The most serious disagreement between the gas-dynamic theory and the measurements is the density ratio, and to a lesser degree the velocity ratio, across the bow shock. For the high Mach number characteristic of the solar wind on the day of the measurements, the theoretical density in the magnetosheath is four times that in the solar wind, yet a jump of only two was observed. Combined with the observed velocity jump, which was not quite as large as predicted by the theory, it is clear that the conservation of normal mass flux across the shock is violated if the shock was aligned along the theoretical direction. In order to conserve mass flux

locally, the shock would have to have been tilted about 15° from the theoretical direction. Since a triple shock crossing was observed, it is plausible to assume that mass flux was conserved locally by such a small tilt. This does not explain the violation of overall mass flux, however, since the observed density jump indicates that the overall flux level in the magnetosheath was a factor of two lower than it should have been, i.e., more particles seemed to be flowing into the magnetosheath than were leaving. It is argued in the Appendix that the solar wind density which should have been measured on the basis of the observed magnetosheath fluxes is outside the experimental error associated with the density which actually was measured. The density ratio across the bow shock has been observed on previous occasions to be lower than that predicted by gas-dynamic theory (Argo et al., 1967), and this discrepancy remains unexplained.

The directional independence of the high energy tail of the velocity distribution near the shock and the evident break in the energy spectrum where these particles join into the Maxwellian distribution indicate that the high energy tail may be due to an effect which is independent from the main flow. Since no alpha particles were detected in the incident solar wind after crossing the bow shock, these high energy particles were not alpha particles unless such particles were in some way generated (or ionized) as the plasma crossed the bow shock.

Solar wind measurements were also made from Pioneer 6 by the Ames Research Center group (ARC) and have been reported by Wolfe et al., (1968). In the following paragraphs we compare the results from the two experiments:

A comparison of the velocity measurements made by the two experiments indicates that the M.I.T. measurements were consistently higher by about 20 km/sec. Since ARC velocities were actually velocities corresponding to the energy of the channel in which the peak flux was detected, the actual convective velocity indicated by the ARC measurements is even more than 20 km/sec lower than those indicated by the M.I.T. measurements, in the magnetosheath (Spreiter et al., 1968). The Ames velocities are well outside the uncertainties in the M.I.T. velocities.

Comparison of the out-of-the-ecliptic flow angle shows a further discrepancy. While this angle was found to be a fairly constant -5° by the M.I.T. experiment, the ARC experiment found that the angle increased from -16° near the magnetopause to 8° near the shock. There is clear disagreement between the experiments in the measurement of this angle, thus care must be taken in drawing firm physical conclusions from the results.

The density pulse observed by ARC at the shock crossing could not be observed by the M.I.T. experiment. During the 50 second period from 1711 +27 sec. UT to 1712 +7 sec. UT, (the time required for one measurement by their experiment) ARC reported a number density increase from 30 to 108 protons/cc. The density jump was caused

primarily by increased current in a low energy channel. In the next 50 second interval they reported interplanetary plasma at a density of 11 protons/cc. Unfortunately, the phasing of the measurements made by the two experiments was such that during the density pulse observations, the M.I.T. experiment was not sampling fluxes at the proper energies to detect such a pulse, although a normal magnetosheath spectrum with a derived density of 21 cm^{-3} was observed between 1712 +5sec. UT and 1712 +17 sec. UT. Therefore, no firm conclusion may be drawn about the existence of this unusual structure from the M.I.T. experiment.

The general success of the gas-dynamic theory in describing the boundary locations and the direction of plasma flow, as well as the trends in the velocity, temperature, and density of the plasma, indicates that some mechanism must be present in the collisionless plasma to shorten the effective mean free path to a distance much less than the size of the magnetosheath.

APPENDIX - ERRORS

The three sources of error which will be discussed here are data quantization, the Maxwellian assumption, and electron contamination of the proton data.

Each current measurement is assigned a data number which is transmitted to the ground. This number does not give the exact current but only indicates that the measured current lies within

a certain current range. The Pioneer 6 instrument was designed so that the current range increased linearly with the current and the widths of the current ranges were chosen so the uncertainty in the current is ±10% for all currents. To obtain some idea of the effect of this uncertainty on the derived plasma parameters, it was necessary to assume a probability distribution of a current in its range. The most realistic distribution is a flat distribution, where any current in the range is equally likely and any current outside the range has zero probability. For computational simplicity, however, a Gaussian distribution, which gave slightly larger errors, was chosen. The most probable current was taken to be the center of the current range, and the standard deviation was assumed to be the ±10% quantization error. With these assumptions, a detailed error analysis was rendered feasibly. The average errors in the derived quantities were estimated to be ±2%, ±10%, and ±10% in the bulk velocity, thermal speed, and density, respectively. These errors are indicated by the error bars in Figure 4. It is important to note than many of the small fluctuations of the results fall within these error bars and that any physical interpretation must take into account this basic uncertainty in the results.

By ignoring the high energy tail, a systematic error was introduced. An estimate of this error shows that the densities and bulk velocities quoted here are roughly 10% and 3% lower than the actual values. The temperature is only a parameter characterizing the energy spread of the observed distributions, thus no attempt was made to estimate the error in the thermal speed due to the high

energy tail.

A high electron flux might be measured as a small current in the proton energy channels in a Faraday cup. This effect has been extensively analyzed (Binsack, 1966) and is especially important in the magnetosheath, where large electron fluxes are observed. The effect was not present here, however, as evidenced by the following observations: As Pioneer 6 passed through the plasma-sheet, copious electron fluxes were observed in all electron channels, while the proton channels measured no currents. In the magnetosheath, large electron fluxes were observed in the anti-solar direction, while again no current was measured in the anti-solar direction proton channels. These observations indicate that there was no electron contamination of the proton data. This conclusion is born out from theoretical calculations. It should be pointed out that the voltage on the suppressor grid was set at a high level specifically to suppress this effect.

In summary, aside from the systematic errors arising from the Maxwellain assumption, the error bars indicated in Figure 4 may be taken as the estimates of experimental error.

Acknowledgments

I am grateful to Dr. Alan Lazarus, without whose encouragement and guidance this work would not have been possible. I am also grateful to the National Science Foundation for its support of me as a National Science Foundation Fellow during this research.

This work was supported by the National Aeronautics and Space Administration under contract NGR 22-009-372.

Bibliography

Argo, H.V., J.R. Asbridge, S.J. Bame, A.J. Hundhausen, and I.B. Strong, "Observations of Solar Wind Plasma Changes across the Bow Shock", J. Geophys. Res., 72, 1989, 1967.

Binsack, J.H., "Plasma Studies with the Imp-2 Satellite", Ph.D. Thesis, M.I.T., 1966. (unpublished).

Hundhausen, A.J., S.J. Bame, and J.R. Asbridge, "Plasma Flow Pattern in the Earth's Magnetosheath", J. Geophys. Res., 74, 2799, 1969.

Lazarus, A.J., H.S. Bridge, and J. Davis, "Preliminary Results from the Pioneer 6 M.I.T. Plasma Experiment", J. Geophys. Res., 71, 3787, 1966.

Lincoln, J.V., "Geomagnetic and Solar Data", J. Geophys. Res., 71, 2411, 1966.

Ness, N.F., C.S. Scearce, and S. Cantarno, "Preliminary Results from the Pioneer 6 Magnetic Field Experiment", J. Geophys. Res., 71, 3305, 1966.

Olbert, S., "Summary of Experimental Results from M.I.T. Detector on IMP-1", Physics of the Magnetosphere, D.Reidel Publishing Co., Holland, 1968.

Spreiter, J.R., A.L. Summers, and A.Y. Alksne, "Hydromagnetic Flow Around the Magnetosphere", Planetary and Space Science, 14, 223, 1966.

Spreiter, J.R., and A.Y. Alksne, "Comparison of Theoretical Predictions of the Flow and Magnetic Fields Exterior to the Magnetosphere with the Observations of Pioneer 6", Planetary and Space Science, 16, 971, 1968.

Spreiter, J.R., and A.Y. Alksne, "Plasma Flow around the Magnetosphere", Reviews of Geophysics, 7, 11, 1969.

Wolfe, J.H., and D.D. McKibbin, "Pioneer 6 Observations of a Steady-State Magnetosheath", Planetary and Space Science, 16, 953, 1968.

Vasyliunas, V.M., "A Survey of Low-Energy Electrons in the Evening Sector of the Magnetosphere with OGO 1 and OGO 3", J. Geophys. Res., 73, 2839, 1968.

Figure Captions

Figure 1. Pioneer 6 trajectory indicating observed boundary crossings and magnetosheath proton flow direction. Also shown are the theoretical position of the magnetopause and the theoretical shock positions for two specific heat ratios, as calculated by Spreiter et al. (1966).

Figure 2. Pioneer 6 energy channels and angular sectors.

Figure 3. Typical magnetosheath energy and angular measurements and the bi-Maxwellain fit. The two thermal speeds are parallel and perpendicular to the bulk velocity, which is within 30° of the magnetic field direction in the magnetosheath.

Figure 4. Pioneer 6 magnetosheath proton observations showing velocity, thermal speed, and number density.

Figure 5. Typical electron energy-angular spectra observed by Pioneer 6 in the near-earth region and a Maxwellian fit. See Figure 6 for the location of regions A, B and C. In region B, the data could be fitted with either

$v_b = 0$, $T_{\perp}/T = 2$ or $v_b = 750$ km/sec., $T_{\perp}/T = 1$.

Figure 6. Pioneer 6 near-Earth electron observations. See text for a discussion of region B.

FIG. 1

PIONEER 6
BOUNDARY CROSSINGS
AND
FLOW DIRECTION

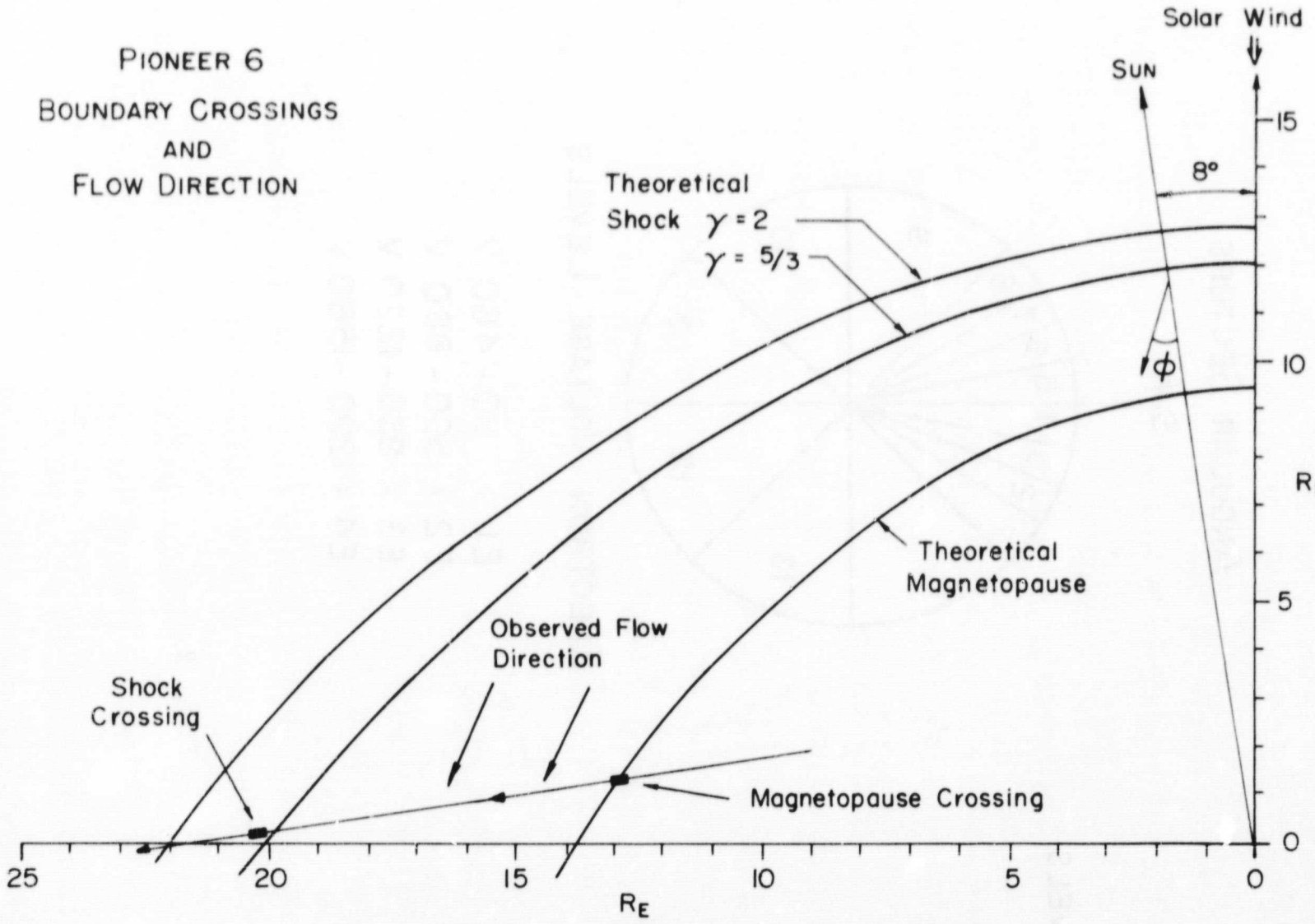

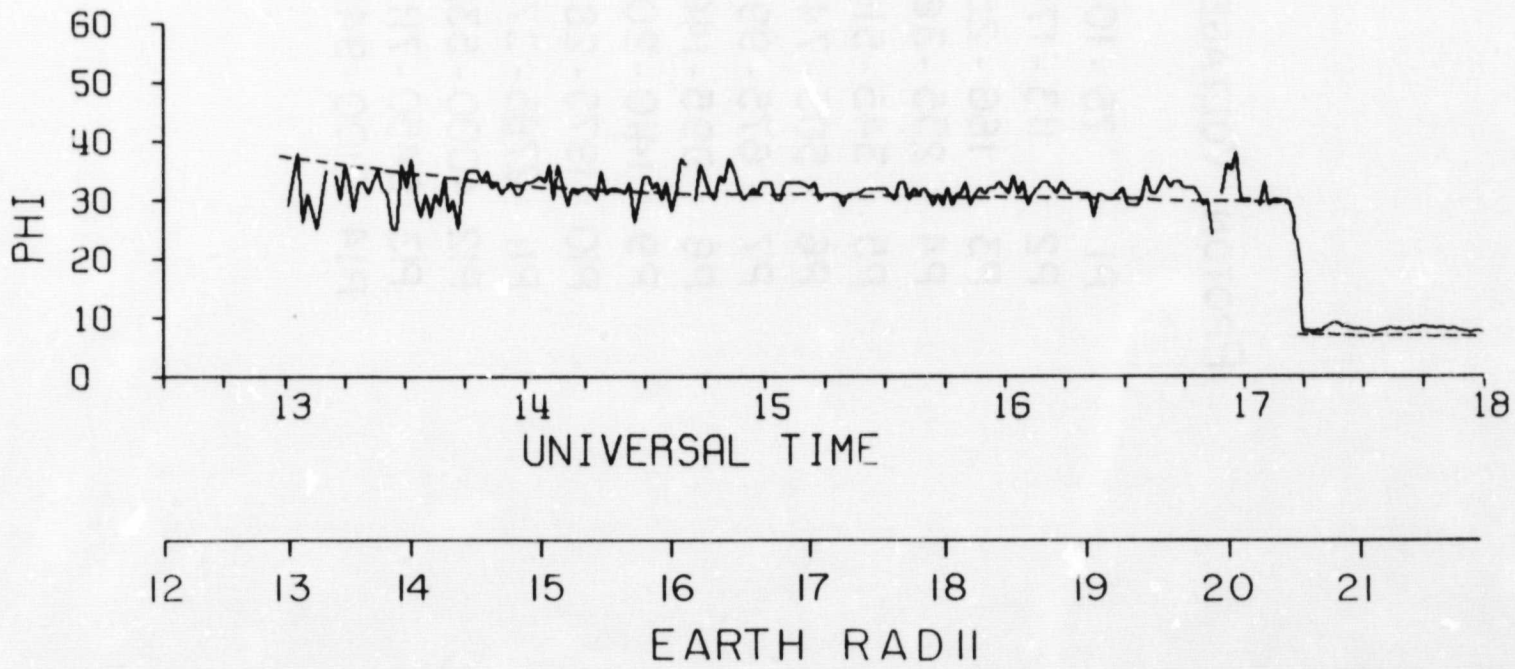

Proton Voltage Levels

P1	: 75 - 100	V
P2	: 113 - 170	V
P3	: 166 - 255	V
P4	: 255 - 365	V
P5	: 345 - 510	V
P6	. 505 - 745	V
P7	. 675 - 990	V
P8	: 995 - 1460	V
P9	: 1410 - 2045	V
P10	: 1975 - 2835	V
P11	: 2785 - 3755	V
P12	: 4000 - 5325	V
P13	: 5450 - 7115	V
P14	: 7100 - 9485	V

Angular Sectors

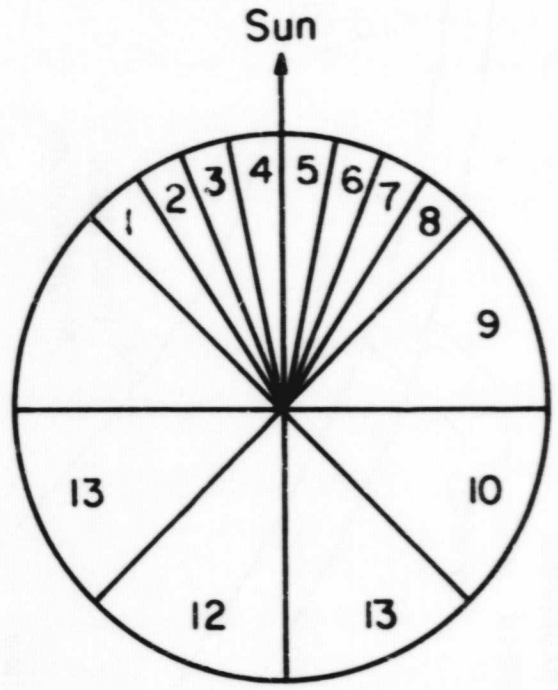

Electron Voltage Levels

E1	: 90 - 460	V
E2	: 500 - 880	V
E3	: 850 - 1220	V
E4	: 1200 - 1580	V

FIG. 2

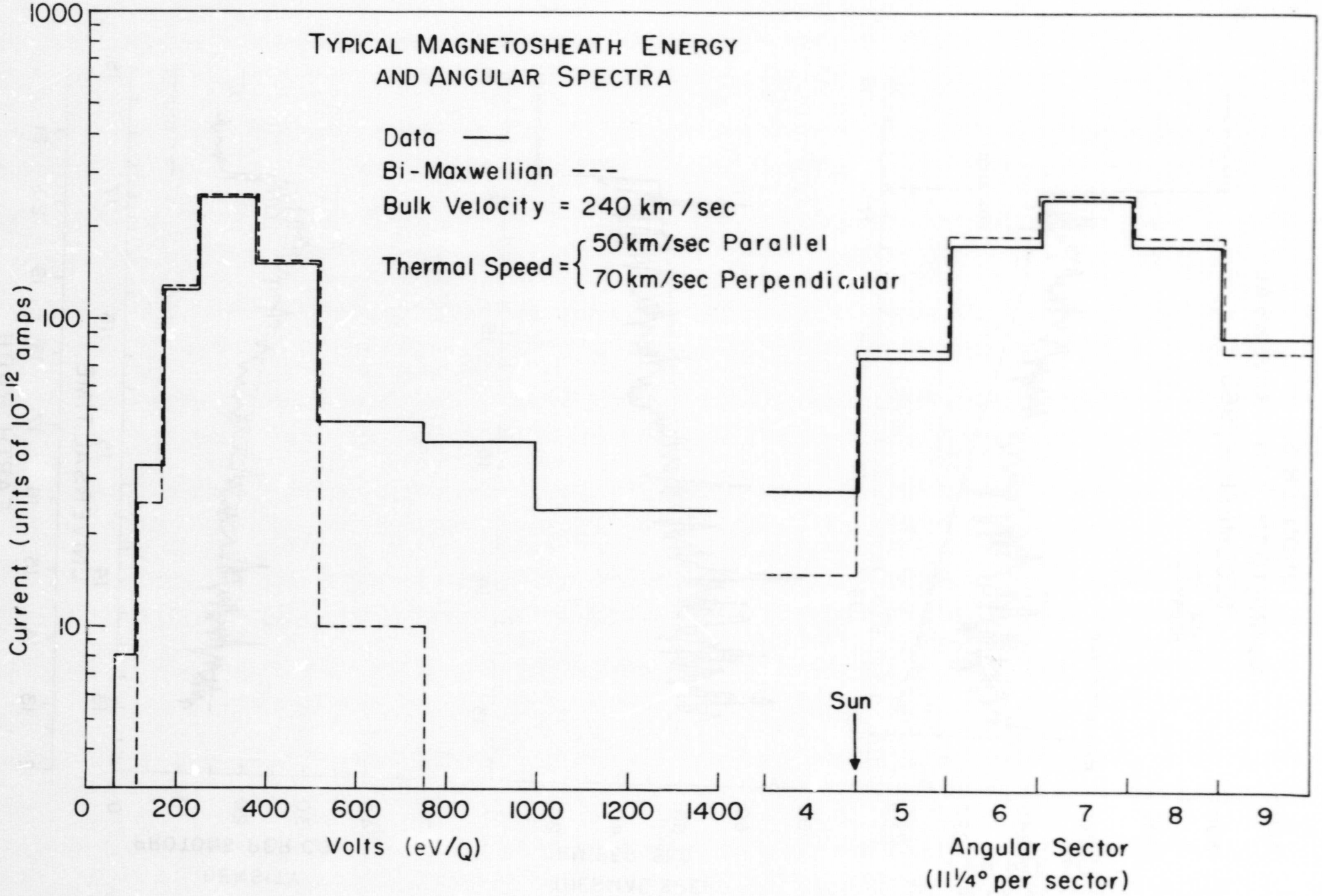
TYPICAL MAGNETOSHEATH ENERGY
AND ANGULAR SPECTRA
Data ——
Bi-Maxwellian ---
Bulk Velocity = 240 km / sec
Thermal Speed = { 50km/sec Parallel
70km/sec Perpendicular
Current (units of 10⁻¹² amps)
1000
100
10
0
200
400
600
800
1000
1200
1400
Volts (eV/Q)
Sun
4
5
6
7
8
9
Angular Sector
(11¼° per sector)

FIG. 3

FIG. 4

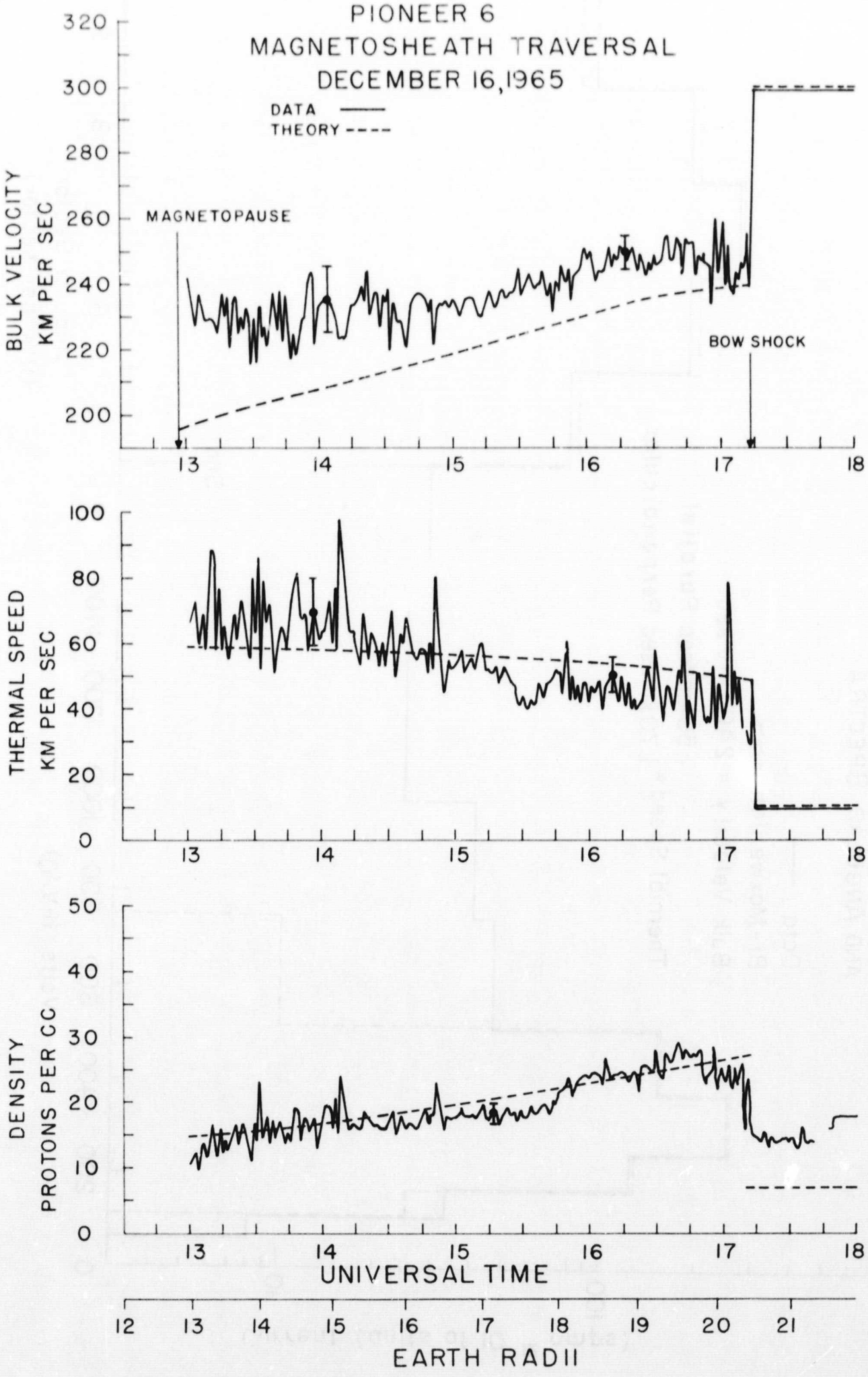
PIONEER 6
MAGNETOSHEATH TRAVERSAL
DECEMBER 16,1965
DATA
THEORY
MAGNETOPAUSE
BOW SHOCK
BULK VELOCITY
KM PER SEC
320
300
280
260
240
220
200
THERMAL SPEED
KM PER SEC
100
80
60
40
20
0
DENSITY
PROTONS PER CC
50
40
30
20
10
0
13
14
15
16
17
18
UNIVERSAL TIME
12
13
14
15
16
17
18
19
20
21
EARTH RADII

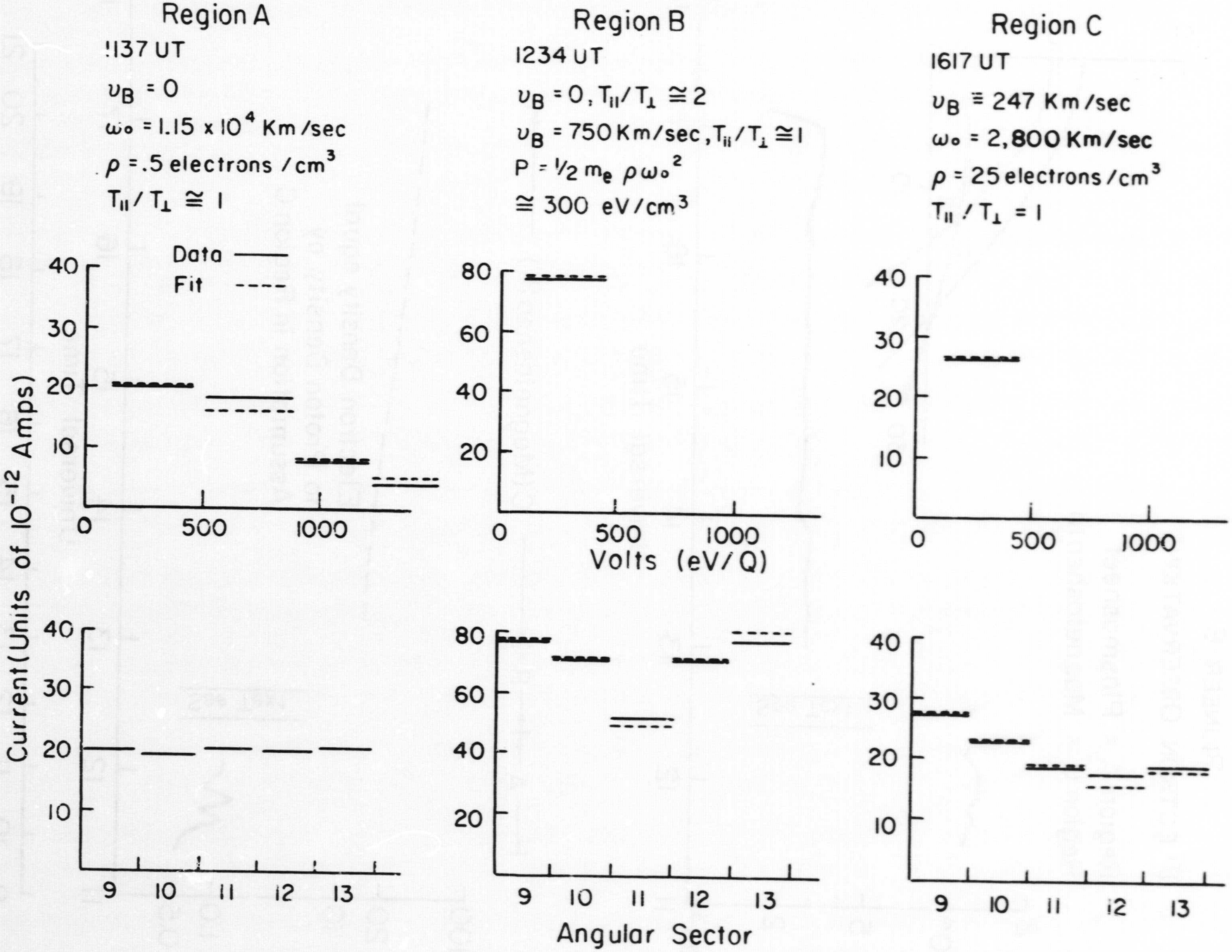

FIG. 5

TYPICAL ELECTRON ENERGY AND ANGULAR SPECTRA

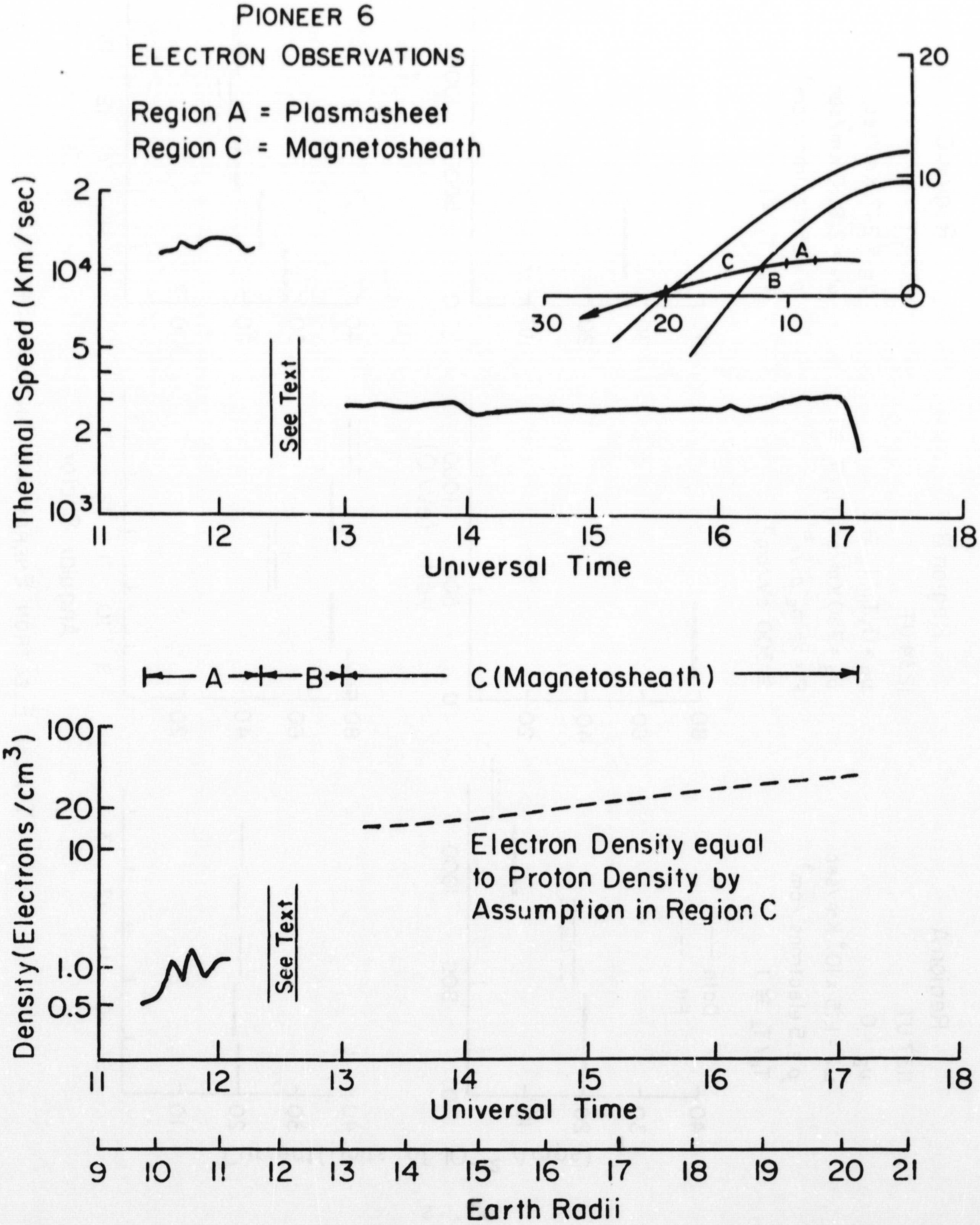
PIONEER 6
ELECTRON OBSERVATIONS
Region A = Plasmasheet
Region C = Magnetosheath
Thermal Speed (Km/sec)
2
10⁴
5
2
10³
See Text
11
12
13
14
15
16
17
18
Universal Time
20
10
30
20
10
C
A
B
A
B
C(Magnetosheath)
Density(Electrons/cm³)
100
20
10
1.0
0.5
See Text
Electron Density equal
to Proton Density by
Assumption in Region C
11
12
13
14
15
16
17
18
Universal Time
9
10
11
12
13
14
15
16
17
18
19
20
21
Earth Radii

FIG. 6